

## Comparison of a Triple Inverted Pendulum Stabilization using Optimal Control Technique

<sup>1</sup>Mustefa Jibril, <sup>1</sup>Messay Tadese and <sup>2</sup>Eliyas Alemayehu Tadese

<sup>1</sup>*School of Electrical and Computer Engineering, Dire Dawa Institute of Technology, Dire Dawa, Ethiopia*

<sup>2</sup>*Faculty of Electrical and Computer Engineering, Jimma Institute of Technology, Jimma, Ethiopia*

**Key words:** Inverted pendulum, linear quadratic regulator, pole placement, strongly, controllers

**Abstract:** In this study, modelling design and analysis of a triple inverted pendulum have been done using MATLAB/Script toolbox. Since, a triple inverted pendulum is highly nonlinear, strongly unstable without using feedback control system. In this study, an optimal control method means a linear quadratic regulator and pole placement controllers are used to stabilize the triple inverted pendulum upside. The impulse response simulation of the open loop system shows us that the pendulum is unstable. The comparison of the closed loop impulse response simulation of the pendulum with LQR and pole placement controllers results that both controllers have stabilized the system but the pendulum with LQR controllers have a high overshoot with long settling time than the pendulum with pole placement controller. Finally, the comparison results prove that the pendulum with pole placement controller improve the stability of the system.

**Corresponding Author:**

Mustefa Jibril

*School of Electrical and Computer Engineering, Dire Dawa Institute of Technology, Dire Dawa, Ethiopia*

Page No.: 60-67

Volume: 14, Issue 6, 2020

ISSN: 1990-7958

International Journal of Electrical and Power Engineering

Copy Right: Medwell Publications

### INTRODUCTION

An inverted pendulum is a pendulum that has its center of mass above its pivot point. It is unstable and without additional assist will fall over. It may be suspended stably in this inverted position by means of the usage of a feedback control system to reveal the angle of the pole and flow the pivot factor horizontally returned beneath the center of mass while it begins to fall over, retaining it balanced<sup>[1]</sup>. The inverted pendulum is a classic problem in dynamics and manage idea and is used as a benchmark for testing control techniques. An inverted pendulum is inherently unstable, and have to be actively balanced with a view to stay upright; this could be accomplished either by applying a torque at the pivot factor with the aid of transferring the pivot point

horizontally as a part of a feedback system, changing the state of rotation of a mass installed at the pendulum on an axis parallel to the pivot axis and thereby generating an internal torque at the pendulum or with the aid of oscillating the pivot factor vertically<sup>[2,3]</sup>. In order to stabilize a pendulum in this inverted position, a feedback control system may be used which monitors the pendulum's attitude and actions the position of the pivot point sideways while the pendulum starts off evolved to fall over, to hold it balanced.

### MATERIALS AND METHODS

**Mathematical modeling:** The pendulum consists of three arms that are hinged by ball bearings and can rotate in the vertical plane. The torques T1 and T2 are the inputs to the

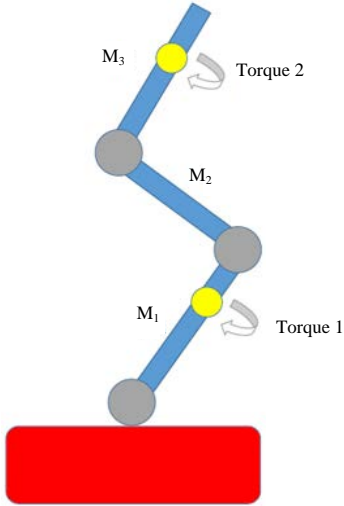


Fig. 1: The triple pendulum

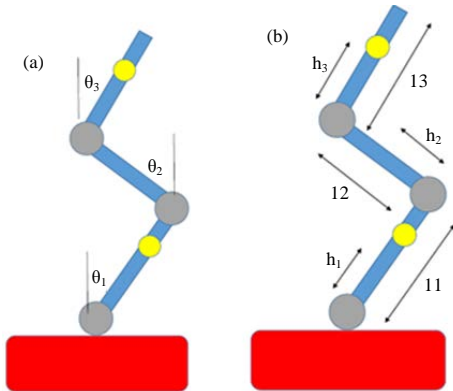


Fig. 2(a, b): System configuration

pendulum with the middle hinge made free for rotation. By controlling the angles of the arms around specified values, the pendulum can be stabilized inversely with the desired angle attitudes. The triple inverted pendulum is shown in Fig. 1.

Let  $T_i$  denote the angle of the  $i$ th arm measured from the vertical axis as shown in Fig. 2. The mathematical modelling of the triple inverted pendulum is derived under the assumption that each arm is a rigid body. Lagrange differential equations is the method used to construct the triple pendulum with a nonlinear vector-matrix differential (Eq. 1) of the form:

$$M(\theta)\ddot{\theta}_i + N\dot{\theta}_i + q_i = GT_j \quad (1)$$

$i = 1, 2, 3$   
 $j = 1, 2$

Where:

$$M(\theta) = \begin{pmatrix} J_1 & I_1 M_2 \cos(\theta_1 - \theta_2) & I_1 M_3 \cos(\theta_1 - \theta_3) \\ I_1 M_2 \cos(\theta_1 - \theta_2) & J_2 & I_2 M_3 \cos(\theta_2 - \theta_3) \\ I_1 M_3 \cos(\theta_1 - \theta_3) & I_2 M_3 \cos(\theta_2 - \theta_3) & J_3 \end{pmatrix} \quad (2)$$

Where:

$$\begin{aligned} M_1 &= m_1 h_1 + m_2 l_1 + m_3 l_1 & J_1 &= I_1 + m_1 h_1^2 + m_2 l_1^2 + m_3 l_1^2 \\ M_2 &= m_2 h_2 + m_3 l_2 & J_2 &= I_2 + m_2 h_2^2 + m_3 l_2^2 \\ M_3 &= m_3 h_3 & \text{and } J_3 &= I_3 + m_3 h_3^2 \end{aligned}$$

The N matrix become:

$$N = \begin{pmatrix} C_1 + C_2 & -C_2 & 0 \\ -C_2 & C_2 + C_3 & -C_3 \\ 0 & -C_3 & C_3 \end{pmatrix} \quad (3)$$

And the q matrix and G matrix are:

$$\begin{aligned} q_1 &= I_1 M_2 \sin(\theta_1 - \theta_2) \dot{\theta}_2^2 + I_1 M_3 \sin(\theta_1 - \theta_3) \dot{\theta}_3^2 - M_1 g \sin(\theta_1) \\ q_2 &= I_1 M_2 \sin(\theta_1 - \theta_2) \dot{\theta}_1^2 + I_2 M_3 \sin(\theta_2 - \theta_3) \dot{\theta}_3^2 - M_2 g \sin(\theta_2) \\ q_3 &= I_1 M_3 \sin(\theta_1 - \theta_3) (\dot{\theta}_1^2 - 2\dot{\theta}_1 \dot{\theta}_3) + \\ & I_2 M_3 \sin(\theta_2 - \theta_3) (\dot{\theta}_2^2 - 2\dot{\theta}_2 \dot{\theta}_3) - M_3 g \sin(\theta_3) \end{aligned}$$

$$G = \begin{pmatrix} 1 & 0 \\ -1 & 1 \\ 0 & -1 \end{pmatrix}$$

After linearization of Eq. 2 under the assumptions of small deviations of the pendulum from the vertical position and of small velocities, one obtains the following Eq. 4:

$$\begin{aligned} M\ddot{\theta}_i + N\dot{\theta}_i + P\theta_i &= GT_m \\ i &= 1, 2, 3 \\ j &= 1, 2 \end{aligned} \quad (4)$$

Where:

$$M = \begin{pmatrix} J_1 & I_1 M_2 & I_1 M_3 \\ I_1 M_2 & J_2 & I_2 M_3 \\ I_1 M_3 & I_2 M_3 & J_3 \end{pmatrix} \quad (5)$$

And:

$$P = \begin{pmatrix} M_1 g & 0 & 0 \\ 0 & -M_2 g & 0 \\ 0 & 0 & -M_3 g \end{pmatrix} \quad (6)$$

The block-diagram of the pendulum system is shown in Fig. 3 and the nominal values of the

Table 1: The description of the system

Symbols	Descriptions
$l_i$	Length of the $i$ th arm
$h_i$	The distance from the bottom to the centre of gravity of the $i$ th arm
$m_i$	Mass of the $i$ th arm
$\theta_i$	Angle of the $i$ th arm from vertical line
$C_i$	Coefficient of viscous friction of the $i$ th hinge
$I_i$	Moment of inertia of the $i$ -th arm around the centre of gravity
$T_j$	Control torque of the $j$ th hinge

Table 2: Nominal values of the parameters

Symbols	Values
$h_1$	0.45 m
$h_2$	0.2 m
$h_3$	0.3 m
$l_1$	0.5 m
$l_2$	0.4 m
$m_1$	3.5 kg
$m_2$	2 kg
$m_3$	2.25 kg
$I_1$	0.55 kg m <sup>2</sup>
$I_2$	0.12 kg m <sup>2</sup>
$I_3$	0.65 kg m <sup>2</sup>
$C_1$	0.07 N m sec
$C_2$	0.03 N m sec
$C_3$	0.009 N m sec

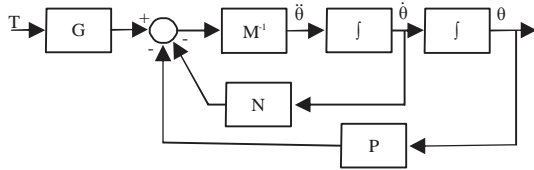


Fig. 3: Block-diagram of the pendulum system

parameters are given in Table 1 and 2. The state space representation of the triple inverted pendulum becomes:

$$\begin{pmatrix} \dot{\theta}_1 \\ \dot{\theta}_2 \\ \dot{\theta}_3 \\ \ddot{\theta}_1 \\ \ddot{\theta}_2 \\ \ddot{\theta}_3 \end{pmatrix} = \begin{pmatrix} -57.75 & -14.42 & -15.82 & -16.26 & -5.5 & -7 \\ -25.3 & -43 & -12.7 & -11 & -13.6 & -5 \\ 178 & 88.6 & 55.6 & 57.3 & 30.2 & 25 \\ 22.9 & -10 & -0.14 & -0.08 & 0.04 & -0.008 \\ -26 & 37.5 & -3.6 & 0.15 & -0.13 & 0.033 \\ -0.83 & -8.2 & 9.25 & -0.01 & 0.04 & -0.02 \end{pmatrix} \begin{pmatrix} \theta_1 \\ \theta_2 \\ \theta_3 \\ \dot{\theta}_1 \\ \dot{\theta}_2 \\ \dot{\theta}_3 \end{pmatrix} + \begin{pmatrix} 1.559 & -0.8 \\ -4 & 3.8 \\ 0.65 & -2.4 \\ 0 & 0 \\ 0 & 0 \\ 0 & 0 \end{pmatrix} \begin{pmatrix} T_1 \\ T_2 \end{pmatrix} = \begin{pmatrix} 1 & 0 & 0 & 0 & 0 & 0 \\ 0 & 1 & 0 & 0 & 0 & 0 \\ 0 & 0 & 1 & 0 & 0 & 0 \\ 0 & 0 & 0 & 1 & 0 & 0 \\ 0 & 0 & 0 & 0 & 1 & 0 \\ 0 & 0 & 0 & 0 & 0 & 1 \end{pmatrix} \begin{pmatrix} \theta_1 \\ \theta_2 \\ \theta_3 \\ \dot{\theta}_1 \\ \dot{\theta}_2 \\ \dot{\theta}_3 \end{pmatrix}$$

**The proposed controllers design**

**LQR controller design:** The principle of most reliable optimal control is involved with working a dynamic system at minimum cost. The case wherein the system dynamics are described via. a fixed of linear differential

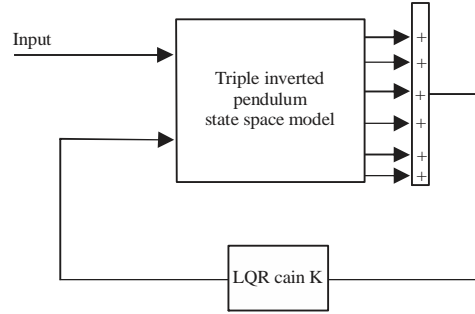


Fig. 4: Block diagram of the triple inverted pendulum with LQR controller

equations and the cost is defined through a quadratic function is referred to as the LQ problem. One of the primary outcomes within the theory is that the solution is furnished with the aid of the Linear Quadratic Regulator (LQR)<sup>[4]</sup>. The block diagram of the triple inverted pendulum with LQR controller is shown below in Fig. 4. In this study, the value of Q and R is chosen as:

$$Q = 10 \begin{pmatrix} 1 & 0 & 0 & 0 & 0 & 0 \\ 0 & 1 & 0 & 0 & 0 & 0 \\ 0 & 0 & 1 & 0 & 0 & 0 \\ 0 & 0 & 0 & 1 & 0 & 0 \\ 0 & 0 & 0 & 0 & 1 & 0 \\ 0 & 0 & 0 & 0 & 0 & 1 \end{pmatrix} \text{ and } R = \begin{pmatrix} 5 & 0 \\ 0 & 5 \end{pmatrix}$$

The value of obtained feedback gain matrix K of LQR is given by:

$$K = \begin{pmatrix} 87.4053 & 32.8355 & 25.6454 & 27.1508 & 11.2981 & 11.1817 \\ 97.7657 & 45.7910 & 30.0834 & 31.2118 & 15.6479 & 12.9896 \end{pmatrix}$$

**Pole placement controller design:** Pole placement is a way employed in feedback control system principle to region the closed-loop poles of a plant in pre-decided locations in the s-plane. Placing poles is proper because the region of the poles corresponds immediately to the eigenvalues of the system which control the traits of the reaction of the system<sup>[5, 6]</sup>. The system ought to be considered controllable on the way to put into effect this technique. The block diagram of the triple inverted pendulum with pole placement controller is shown in Fig. 5. The state equations for the closed-loop system of Fig. 5 can be written by inspection as:

$$\begin{aligned} \dot{x} &= Ax + Bu = Ax + B(-Kx) = (A - BK)x \\ y &= Cx \end{aligned} \tag{7}$$

The poles for this system is chosen as:

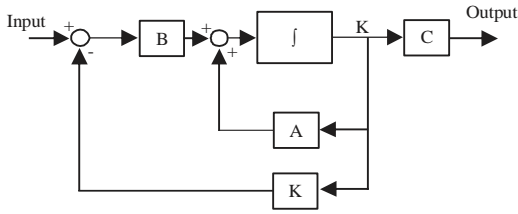


Fig. 5: Block diagram of the triple inverted pendulum with pole placement controller

$$P = [-1, -2, -3, -4, -5, -6]$$

Solving using MATLAB the robust pole placement algorithm gain will be:

$$K = \begin{bmatrix} 19329 & 8885 & 7472 & 11601 & 5861 & 6699 \\ 23483 & 10820 & 9086 & 14362 & 7268 & 8307 \end{bmatrix}$$

### RESULTS AND DISCUSSION

**Controllability and observability of the pendulum:** A system (state space representation) is controllable iff the controllable matrix  $C = [B \ AB \ A^2B, \dots, A^{n-1}B]$  has rank  $n$  where  $n$  is the number of degrees of freedom of the system.

In our system, the controllable matrix  $C = [B \ AB \ A^2B \ A^3B \ A^4B \ A^5B]$  has rank 6 which the degree of freedom of the system. So, the system is controllable. A system (state space representation) is Observable iff the Observable matrix  $D = [C \ CA \ CA^2 \dots \ CA^{n-1}]^T$  has a full rank  $n$ . In our system, the Observable matrix  $D = [C \ CA \ CA^2 \ CA^3 \ CA^4 \ CA^5]^T$  has a full rank of 6. So, the system is Observable.

**Open loop impulse response of the triple inverted pendulum:** The open loop simulation for a 1 Nm impulse input of torque 1 for angular displacement 1-3 and for angular velocity 1-3 is shown in Fig. 6-11 and for torque 2 input the angular displacement 1-3 and for angular velocity 1-3 is shown in Fig. 12-17, respectively. As we seen from the Figures above the angular displacements and the angular velocities are unstable<sup>[7]</sup>.

**Comparison of the triple inverted pendulum with LQR and pole placement controllers for impulse input signal:** The comparison of the triple inverted pendulum with LQR and pole placement controller for a 1 Nm impulse input of torque 1 for angular displacement 1-3 and for angular velocity 1-3 is shown in Fig. 18-23 and for torque 2 input the angular displacement 1-3 and for angular velocity 1-3 is shown in Fig. 24-29, respectively.

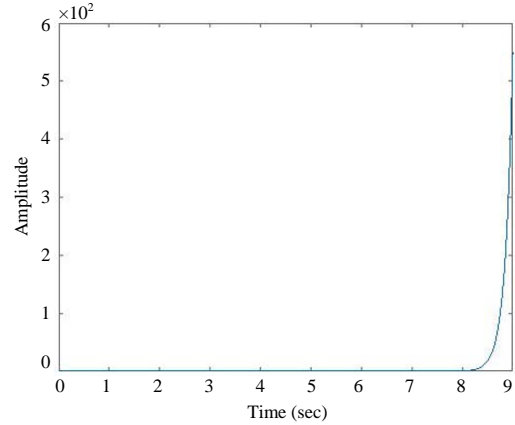


Fig. 6: Response of  $\theta_1$ ; for a 1 Nm impulse input of T1

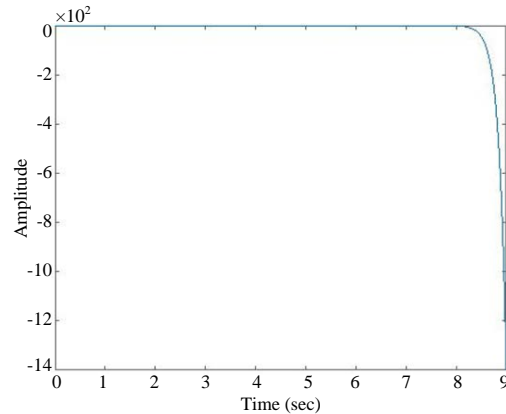


Fig. 7: Response of  $\theta_2$ ;  $\theta_1$  for a 1 Nm impulse input of T1

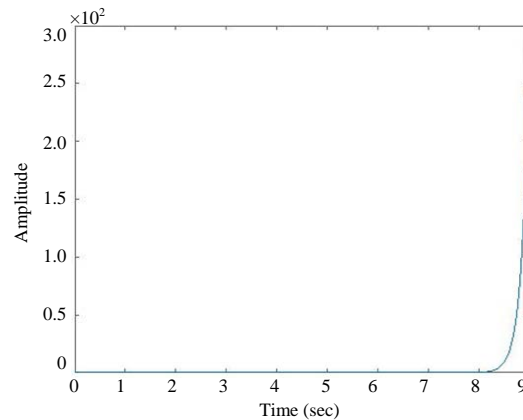


Fig. 8: Response of  $\theta_3$ ;  $\theta_1$  for a 1 Nm impulse input of T1

As we seen from Figure 18, 19 and 20, for the impulse signal the angles starts to increase and returns to

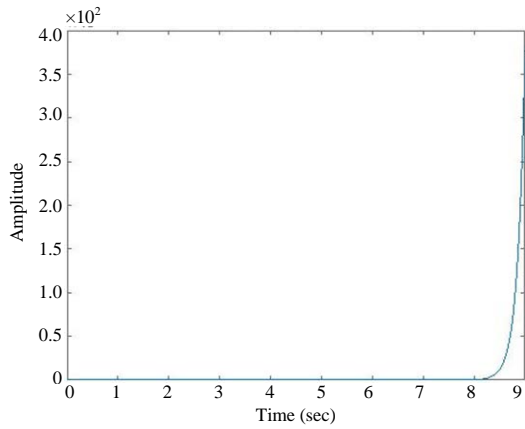


Fig. 9: Response of  $\theta_1; \theta_1$  for a 1 Nm impulse input of T1

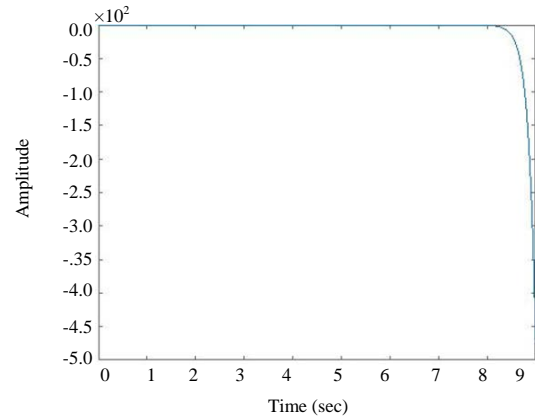


Fig. 12: Response of  $\theta_1; \theta_1$  for a 1 Nm impulse input of T2

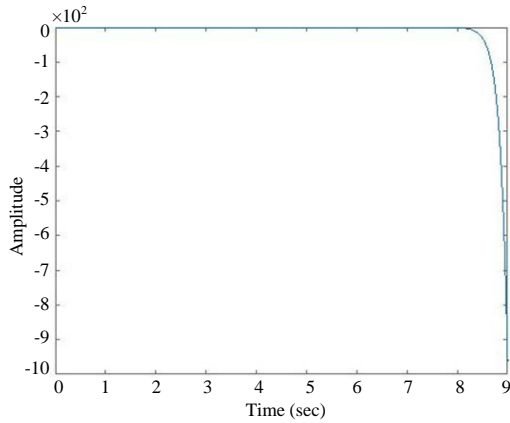


Fig. 10: Response of  $\theta_2; \theta_1$  for a 1 Nm impulse input of T1

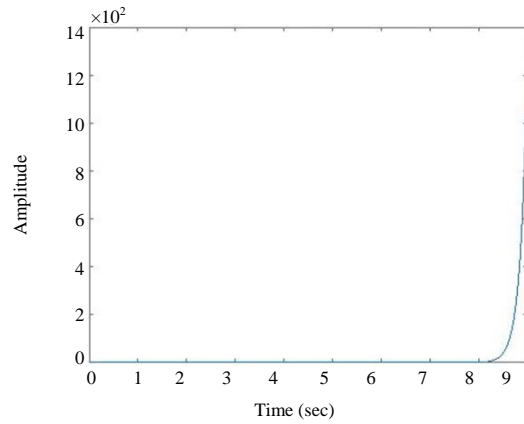


Fig. 13: Response of  $\theta_2; \theta_1$  for a 1 Nm impulse input of T2

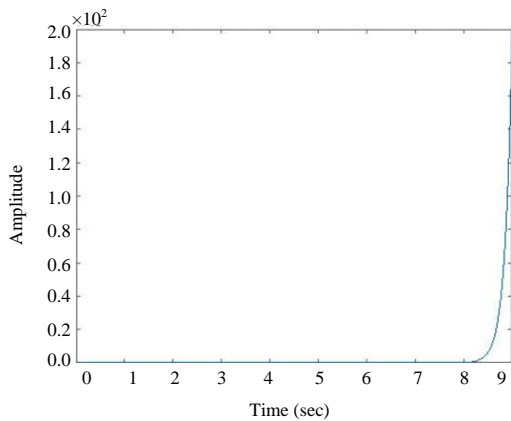


Fig. 11: Response of  $\theta_3; \theta_1$  for a 1 Nm impulse input of T1

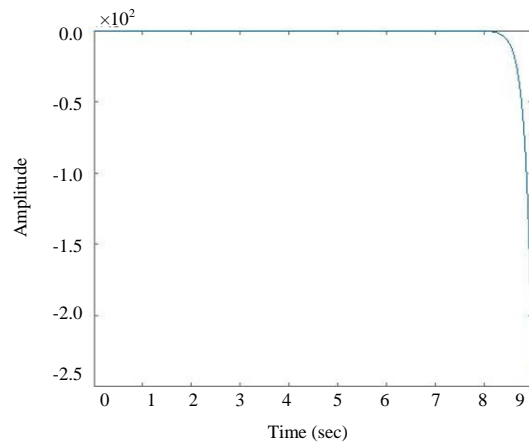


Fig. 14: Response of  $\theta_3; \theta_1$  for a 1 Nm impulse input of T2

$0^\circ$  for the two controllers but the pendulum with LQR controller has a high overshoot with more settling time

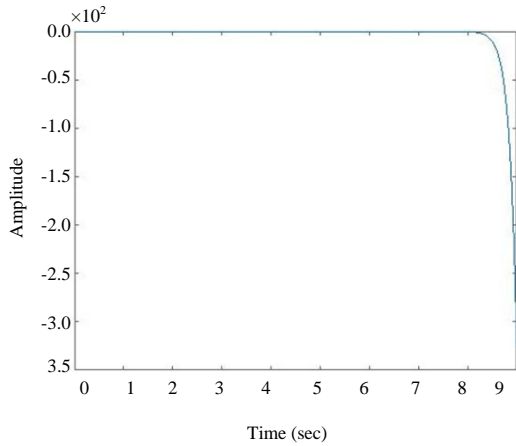


Fig. 15: Response of  $\theta_1$ ;  $\theta_1$  for a 1 Nm impulse input of T2

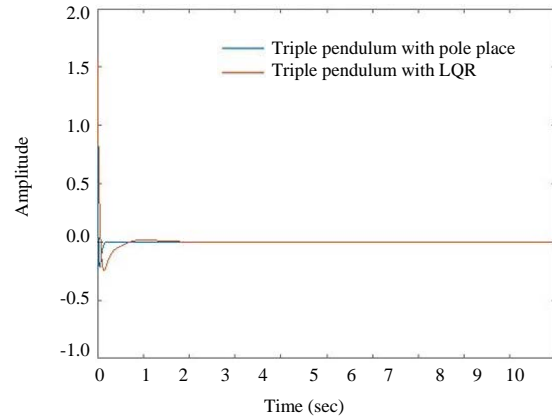


Fig. 18: Response of  $\theta_1$ ;  $\theta_1$  for a 1 Nm impulse input of T1

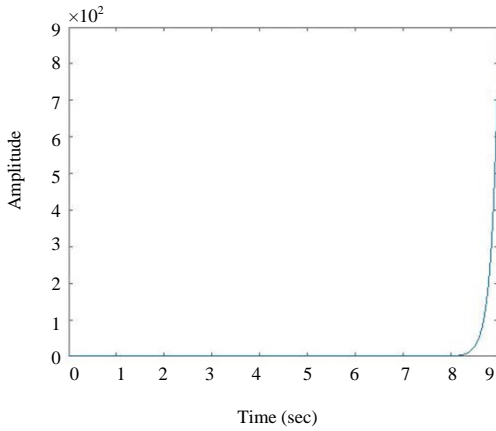


Fig. 16: Response of  $\theta_2$ ;  $\theta_1$  for a 1 Nm impulse input of T2

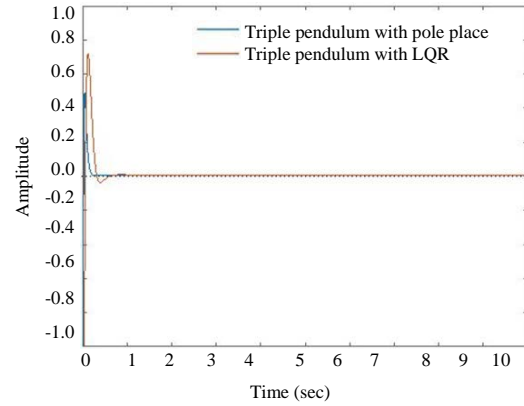


Fig. 19: Response of  $\theta_2$ ;  $\theta_1$  for a 1 Nm impulse input of T1

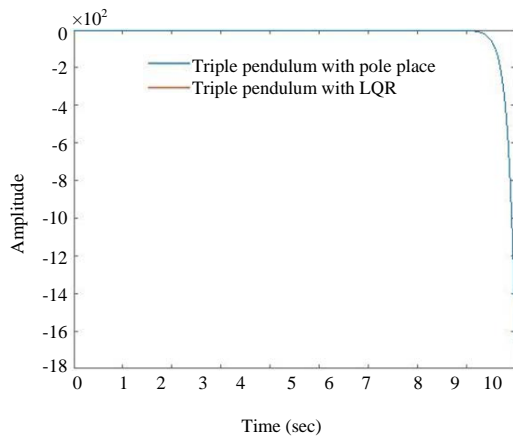


Fig. 17: Response of  $\theta_3$ ;  $\theta_1$  for a 1 Nm impulse input of T2

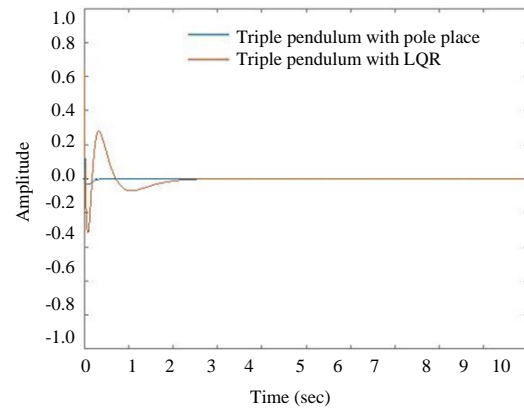


Fig. 20: Response of  $\theta_3$ ;  $\theta_1$  for a 1 Nm impulse input of T1

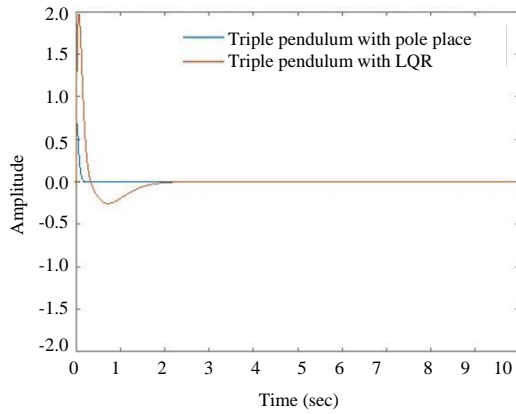


Fig. 21: Response of  $\theta_1$ ;  $\dot{\theta}_1$  for a 1 Nm impulse input of T1

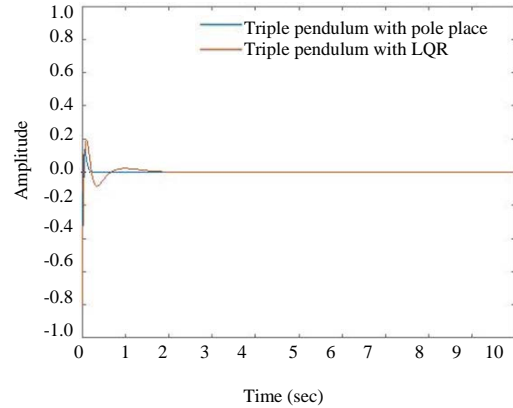


Fig. 24: Response of  $\theta_1$ ;  $\dot{\theta}_1$  for a 1 Nm impulse input of T2

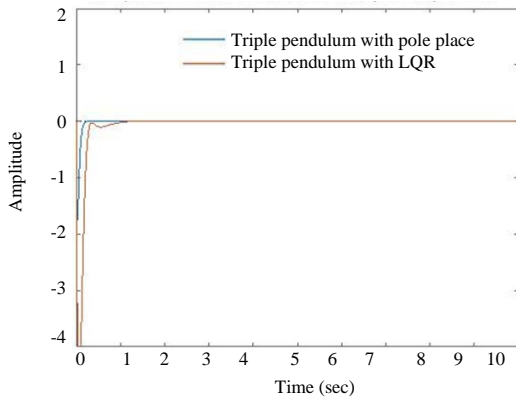


Fig. 22: Response of  $\theta_2$ ;  $\dot{\theta}_1$  for a 1 Nm impulse input of T1

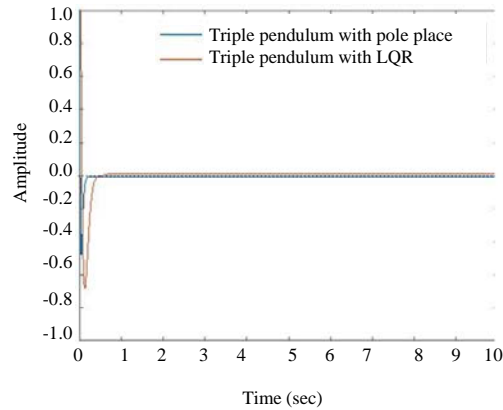


Fig. 25: Response of  $\theta_2$ ;  $\dot{\theta}_1$  for a 1 Nm impulse input of T2

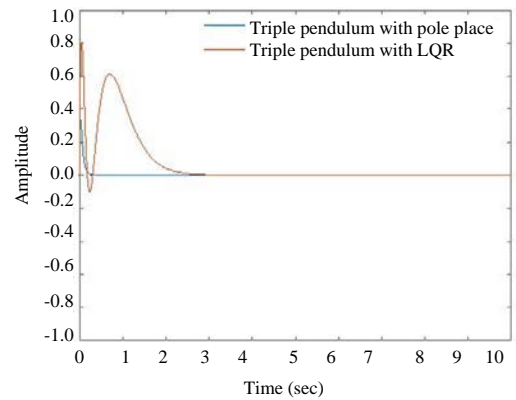


Fig. 23: Response of  $\theta_3$ ;  $\dot{\theta}_1$  for a 1 Nm impulse input of T1

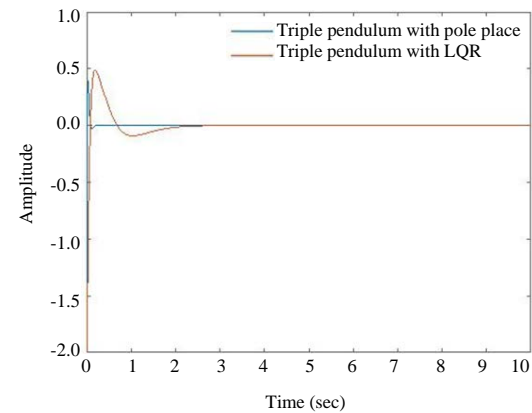


Fig. 26: Response of  $T \theta_3$ ;  $\dot{\theta}_1$  for a 1 Nm impulse input of T2

than the pendulum with pole placement controller. Figure 21-23 for the impulse signal the angular velocities

starts to increase and returns to zero for the two controllers but the pendulum with LQR controller

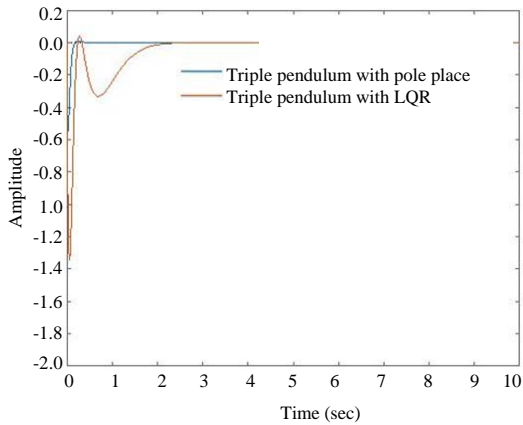


Fig. 27: Response of  $\theta_1$  Dot;  $\theta_1$  for a 1 Nm impulse input of T2

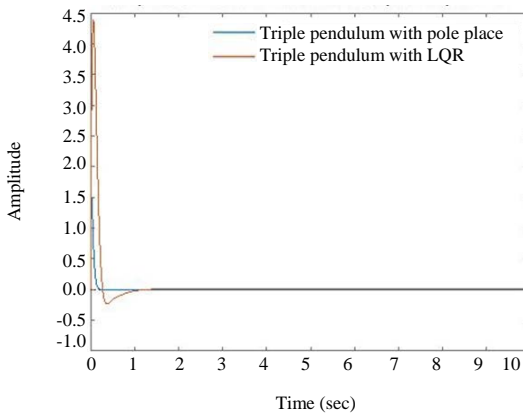


Fig. 28: Response of  $\theta_2$  Dot;  $\theta_1$  for a 1 Nm impulse input of T2

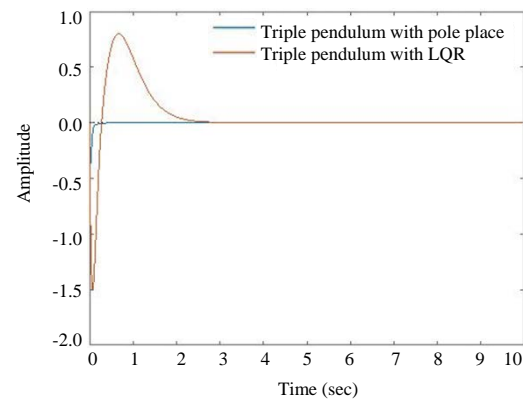


Fig. 29: Response of  $\theta_3$  Dot;  $\theta_1$  for a 1 Nm impulse input of T2

has a high overshoot with more settling time than the pendulum with pole placement controller. As we seen from Fig. 24-26, for the impulse signal the angles starts to increase and returns to zero degree for the two controllers but the pendulum with LQR controller has a high overshoot with more settling time than the pendulum with pole placement controller.

As we seen from Fig. 27-29, for the impulse signal the angular velocities starts to increase and returns to zero for the two controllers but the pendulum with LQR controller has a high overshoot with more settling time than the pendulum with pole placement controller.

## CONCLUSION

In this study, stabilization of the triple inverted pendulum with LQR and pole placement controller have been analyzed simulated and compared successfully. The open loop simulation prove that the system is not stable without feedback control system. Comparison of the proposed controllers for an impulse input have been done and the system with pole placement controller improves the stability of the system.

## REFERENCES

01. Tang, Y., D. Zhou and W. Jiang, 2016. A new fuzzy-evidential controller for stabilization of the planar inverted pendulum system. PloS One, Vol. 11, No. 8. 10.1371/journal.pone.0160416.
02. Jibril, M., 2020. Robust control theory based performance investigation of an inverted pendulum system using simulink. Int. J. Adv. Res. Innovative Ideas Educ., 6: 808-814.
03. Huang, X., F. Wen and Z. Wei, 2018. Optimization of triple inverted pendulum control process based on motion vision. EURASIP J. Image Video Process., Vol. 2018. 10.1186/s13640-018-0294-6.
04. Chen, W. and N. Theodomile, 2016. Simulation of a triple inverted pendulum based on fuzzy control. World J. Eng. Technol., 4: 267-272.
05. Pristovani, R.D., D.R. Sanggar and P. Dadet, 2018. Implementation of push recovery strategy using triple linear inverted pendulum model in T-flow humanoid robot. IOP. J. Phys. Conf. Ser., 1007: 1-13.
06. Dan, Y., P. Xu, Z. Tan and Z. Li, 2015. Multi-mode control based on HSIC for double pendulum robot. J. Vibroengineering, 17: 3683-3692.
07. Rohan, A., M. Rabah, K.H. Nam and S.H. Kim, 2018. Design of fuzzy logic based controller for gyroscopic inverted pendulum system. Int. J. Fuzzy Logic Intell. Syst., 18: 58-64.